THE JOURNAL OF BIOLOGICAL CHEMISTRY VOL. 289, NO. 8, pp. 5228–5239, February 21, 2014

Mycothiol/Mycoredoxin 1-dependent Reduction of the Peroxiredoxin AhpE from *Mycobacterium tuberculosis*[*]

Received for publication, August 13, 2013, and in revised form, December 23, 2013 Published, JBC Papers in Press, December 30, 2013, DOI 10.1074/jbc.M113.510248

Martín Hugo[‡§1], Koen Van Laer[¶‖2], Aníbal M. Reyes[‡§], Didier Vertommen[‡‡3], Joris Messens[¶‖**4], Rafael Radi[‡§], and Madia Trujillo[‡§5]**

*From the [‡]Departamento de Bioquímica and [§]Center for Free Radical and Biomedical Research, Universidad de la República, 11800 Montevideo, Uruguay, the [¶]Structural Biology Research Center, Vlaams Instituut voor Biotechnologie (VIB), 1050 Brussels, Belgium, the [‖]Brussels Center for Redox Biology, 1050 Brussels, Belgium, the **Structural Biology Brussels, Vrije Universiteit Brussel (VUB), 1050 Brussels, Belgium, and the [‡‡]de Duve Institute, Université Catholique de Louvain, 1200 Brussels, Belgium*

Background: Mycothiol, the major low-molecular weight thiol of *Mycobacterium tuberculosis*, is important for peroxide detoxification and virulence.
Results: Mycothiol, together with mycoredoxin-1, a glutaredoxin-like protein, reduces the one-cysteine peroxiredoxin AhpE from the bacterium.
Conclusion: *Mycobacterium tuberculosis* AhpE is a mycothiol/mycoredoxin-1-dependent peroxidase.
Significance: Our results provide the first molecular link between a thiol-dependent peroxidase and the mycothiol/mycoredoxin-1 pathway in Mycobacteria.

***Mycobacterium tuberculosis* (*M. tuberculosis*), the pathogen responsible for tuberculosis, detoxifies cytotoxic peroxides produced by activated macrophages. *M. tuberculosis* expresses alkyl hydroxyperoxide reductase E (AhpE), among other peroxiredoxins. So far the system that reduces AhpE was not known. We identified *M. tuberculosis* mycoredoxin-1 (*Mt*Mrx1) acting in combination with mycothiol and mycothiol disulfide reductase (MR), as a biologically relevant reducing system for *Mt*AhpE. *Mt*Mrx1, a glutaredoxin-like, mycothiol-dependent oxidoreductase, directly reduces the oxidized form of *Mt*AhpE, through a protein mixed disulfide with the N-terminal cysteine of *Mt*Mrx1 and the sulfenic acid derivative of the peroxidatic cysteine of *Mt*AhpE. This disulfide is then reduced by the C-terminal cysteine in *Mt*Mrx1. Accordingly, *Mt*AhpE catalyzes the oxidation of wt *Mt*Mrx1 by hydrogen peroxide but not of *Mt*Mrx1 lacking the C-terminal cysteine, confirming a dithiolic mechanism. Alternatively, oxidized *Mt*AhpE forms a mixed disulfide with mycothiol, which in turn is reduced by *Mt*Mrx1 using a monothiolic mechanism. We demonstrated the H_2O_2-dependent NADPH oxidation catalyzed by *Mt*AhpE in the presence of MR, Mrx1, and mycothiol. Disulfide formation involving mycothiol probably competes with the direct reduction by *Mt*Mrx1 in aqueous intracellular media, where mycothiol is present at millimolar concentrations. However, *Mt*AhpE was found to be associated with the membrane fraction, and since mycothiol is hydrophilic, direct reduction by *Mt*Mrx1 might be favored. The results reported herein allow the rationalization of peroxide detoxification actions inferred for mycothiol, and more recently, for Mrx1 in cellular systems. We report the first molecular link between a thiol-dependent peroxidase and the mycothiol/Mrx1 pathway in Mycobacteria.**

Mycobacterium tuberculosis is the causative agent of tuberculosis disease (TB).[6] Despite the efforts made during the last two decades to reduce new TB cases and deaths, the global burden of the disease remains enormous (1). Moreover, the emergency of multi- and extensively drug resistant strains underlines the need for the urgent development of new therapeutic approaches (1, 2). However, since many aspects of the pathogenic mechanisms and virulence of *M. tuberculosis* are still unknown, the identification of novel drug targets has been very challenging (2).

M. tuberculosis survives inside the hostile environment of host cells with diverse defense strategies. These antioxidant defenses allow the pathogen to detoxify reactive oxygen and nitrogen species formed by activated macrophages (3–5). One particular feature of the antioxidant systems of *M. tuberculosis* as well as other Actinomycetes is the absence of glutathione,

* This work was supported by grants from the National Institutes of Health (NIH) and Universidad de la República (to R. R.), agentschap voor innovatie door Wetenschap en technologie (IWT) (to K. V. L.), the Vlaams Instituut voor Biotechnologie (VIB) and the FWO (Project Grant G.0305.12) (to J. M.), Agencia Nacional de Investigación e Innovación (ANII, Uruguay, FCE_2011_1_5706) (to M. T.). We thank EMBO for the Visiting Grant 439-2011 (to M. H.).
[1] Supported in part by a PhD fellowship from ANII.
[2] Recipient of an IWT PhD fellowship.
[3] Collaborateur Logistique at FRS-FNRS, Belgium.
[4] Group leader at the VIB. To whom correspondence may be addressed: Structural Biology Research Center, Oxidative Stress Signaling Lab., Vlaams Instituut voor Biotechnologie (VIB), Vrije Universiteit Brussel (VUB), Pleinlaan 2, 1050 Brussels, Belgium. Tel.: +32-2-6291992; Fax: +32-2-6291963; E-mail: joris.messens@vib-vub.be.
[5] To whom correspondence may be addressed: Departamento de Bioquímica and Center for Free Radical and Biomedical Research, Universidad de la República, Avenida General Flores 2125, 11800 Montevideo, Uruguay. Tel.: 598-2-9249561; Fax: 598-2-9249563; E-mail: madiat@fmed.edu.uy.

[6] The abbreviations used are: TB, tuberculosis disease; AhpE, alkyhydroperoxide reductase E; β-ME, β-mercaptoethanol; DTPA, diethylene triamine pentaacetic acid; DTT, dithiothreitol; NEM, *N*-ethylmaleimide; H_2O_2, hydrogen peroxide; HRP, horseradish peroxidase; Mrx1, mycoredoxin-1 from *Mycobacterium tuberculosis*; MSH, mycothiol; MR, mycothiol disulfide reductase; PEG-maleimide, methoxypolyethylene glycol maleimide; TCA, trichloroacetic acid.

and the presence of millimolar concentrations of 1-D-*myo*-inosityl 2-(*N*-acetyl-L-cysteinyl)amido-2-deoxy-α-D-glucopyranoside (mycothiol or MSH) (6,7) as the main low molecular weight thiol. Mycothiol is maintained in its reduced state by a mycothiol disulfide reductase that uses NADPH as electron donor (8) and plays a role in peroxide detoxification *in vivo*, as evidenced by the increased susceptibility to hydrogen peroxide (H_2O_2), menadione and *tert*-butyl hydroperoxide in *M. smegmatis* and *M. tuberculosis* mutant strains disrupted in the genes required for mycothiol biosynthesis (9–11). Compensatory overexpression of an organic hydroperoxide resistance protein (Ohr) in *M. smegmatis* lacking MSH suggests the existence of a MSH-dependent organic hydroperoxide peroxidase (12). Although these data are only indirect evidence for the presence of a MSH-dependent peroxidase in these bacteria, the molecular link between MSH and peroxidase activity has not been clearly established yet, and purified peroxidases studied so far failed in using MSH as reducing substrate (13). Despite the absence of glutathione, the *M. tuberculosis* genome encodes different glutaredoxin-like proteins (14). Among them, mycoredoxin 1 (*Mt*Mrx1 EC 1.20.4.3) has recently been described as a 10-kDa protein with a CGYC catalytic motif that accepts electrons from MSH and reduces MSH-containing mixed disulfides by a monothiolic mechanism (7, 15). Strains of *M. smegmatis* lacking Mrx1 are more susceptible to different forms of oxidative stress (15). Moreover, in *Corynebacterium glutamicum*, this protein participates in the arsenate resistance system by reducing the mycothiol arsenate adduct (16). More recently, twenty-five proteins of *C. glutamicum* including thiol peroxidase (TPx) were found mycothiolated under hypochloric stress conditions (17). The *S*-mycothiolation of Tpx inhibits its peroxidase activity, but could be restored after treatment with *Cg*Mrx1. So far no *Mt*Mrx1-dependent protein reduction has been described in Mycobacteria. *M. tuberculosis* expresses a heme-dependent peroxidase (catalase peroxidase, KatG, EC 1.11.1.6) and several thiol-dependent peroxidases of the peroxiredoxin (Prx, EC 1.11.1.15) type, including alkyl hydroperoxide reductase C, TPx, two bacterioferritin comigratory proteins (Bcp andBcpB) and alkyl hydroperoxide reductase E (*Mt*AhpE) (13, 18).[7] As a one-cysteine peroxidase, *Mt*AhpE lacks a resolving cysteine. However, the structure and sequence of *Mt*AhpE show greater similarity with two-cysteine Prxs than with other one-cysteine Prxs, and is considered as the prototype of a novel Prx subfamily (19–21). We have previously investigated the peroxidase activity of *Mt*AhpE, the only Prx of the AhpE subfamily to be functionally characterized. It is a broad-spectrum peroxidase with higher catalytic efficiency for fatty acid hydroperoxides and peroxynitrite than for H_2O_2. Upon reaction with the peroxide substrate (ROOH), the thiolate form of the peroxidatic cysteine (C_P) is oxidized to a sulfenic acid (22, 23) as in Equation 1.

$$\text{AhpE-S}^- + \text{ROOH} \rightarrow \text{AhpE-SOH} + \text{RO}^- \qquad \text{(Eq. 1)}$$

[7] List of Gen Accession numbers (TubercuList) of peroxidases and mycoredoxin 1 from *M. tuberculosis*: catalase peroxidase, Rv1908; alkyl hydroperoxide reductase C, Rv2428; thioredoxin peroxidase, Rv1932; bacterioferritin comigratory protein, Rv2521; bacterioferritin comigratory protein B, Rv1608c; alkyl hydroperoxide reductase E, Rv2238c; mycoredoxin 1, Rv3198A.

*Mt*AhpE catalytically reduces hydrogen peroxide (H_2O_2) in the presence of dithiothreitol (DTT) or thionitrobenzoate (TNB) as reducing agents (22). However, the physiological reducing substrate(s) for this enzyme (as well as for AhpE-like Prxs from several other bacteria) is/are still unknown. Neither *N*-acetylcysteine nor glutathione reduced oxidized *Mt*AhpE, but led to the formation of mixed disulfides (22) in Equation 2.

$$\text{AhpE-SOH} + \text{RS}^- \rightarrow \text{AhpE-SS-R} + \text{OH}^- \qquad \text{(Eq. 2)}$$

Similar disulfide formation involving the main low molecular weight thiol of the bacteria, mycothiol, had not been addressed so far.

Herein, we report that *Mt*Mrx1 and *Mt*Mrx1 in combination with mycothiol acts as a reducing substrate for *Mt*AhpE. Our data not only constitute the first report for biologically relevant routes of reduction for an AhpE-like Prx, but also describe the first acceptor for the electrons provided by a mycoredoxin in Mycobacteria. We also propose a functional link between the mycothiol/mycoredoxin-1 pathway and the bacterial peroxide detoxification systems, which helps to rationalize the increased peroxide-dependent cytotoxicity in Mycobacteria with a reduced MSH content (9–11).

EXPERIMENTAL PROCEDURES

Chemicals—H_2O_2 was from Mallinckrodt Chemicals. Dithiotreitol (DTT), *N*-ethylmaleimide (NEM), β-mercaptoethanol (β-ME), diethylenetriaminepentaacetic acid (DTPA), methoxypolyethylene glycol maleimide (PEG-maleimide), sodium dodecyl sulfate (SDS), 4-(2-hydroxyethyl)piperazine-1-ethanesulfonic acid, *N*-(2-hydroxyethyl) piperazine-*N*′-(2-ethanesulfonic acid), (HEPES), and horseradish peroxidase (HRP) were from Sigma. β-Nicotinamide adenine dinucleotide phosphate reduced tetrasodium salt (NADPH) was from Applichem. PageRuler™ prestained protein ladder was from Fermentas. Amplex® red was from Invitrogen. All other reagents were obtained from standard commercial sources and used as received. All experiments were performed in 100 mM phosphate buffer, 0.1 mM DTPA, pH 7.4, and 25 °C, except if otherwise indicated.

Mycothiol Purification—MSH was purified from *M. smegmatis* as described (7).

Protein Expression and Purification—Mycothiol disulfide reductase from either *M. tuberculosis* (*Mt*MR) or *C. glutamicum* (*Cg*MR) were expressed and purified as previously described (15, 16). The *Cg*MR preparation was more robust and active compared with *Mt*MR, and therefore it was preferentially utilized. *Mt*AhpE was expressed in *Escherichia coli* BL21 (DE3) (expression vector pDEST17) as a recombinant His-tagged protein and purified as previously described (22). The enzyme was stored at −80 °C under argon atmosphere. Wild type *Mt*Mrx1 (*Mt*Mrx1wt) and a mutant form at the second cysteine residue (*Mt*Mrx1CXXA) were expressed in *Escherichia coli* BL21 Star and purified as previously described (15). Following the immobilized metal ion affinity chromatography step, *Mt*Mrx1CXXA was further purified by size exclusion chromatography using a Superdex 75 10/300 column in 100 mM phosphate buffer, 0.1 mM DTPA, pH 7.4. Both *Mt*Mrx1wt and *Mt*Mrx1CXXA were stored at −20 °C in the presence of 5 mM DTT. Excess reduc-

tant was removed by gel filtration using a HiTrap desalting column (Amersham Bioscience) with UV-vis detection at 280 nm immediately before use.

Protein Thiol Reduction—*Mt*AhpE was reduced before use by incubation with 1 mM DTT for 30 min at 4 °C. Excess reductant was removed from all proteins immediately before use by gel filtration as above indicated.

Peroxide, Protein, and Thiol Quantitation—The concentration of H_2O_2 stock solutions was measured at 240 nm (λ_{240} = 43.6 $M^{-1}cm^{-1}$) (24). *Mt*AhpE, *Mt*Mrx1wt, and *Mt*Mrx1CXXA concentrations were determined spectrophotometrically at 280 nm, using molar absorption coefficients of 23,950 (22), 9,974 and 9,942 $M^{-1}\,cm^{-1}$, respectively, calculated from amino acidic composition. Protein concentrations calculated refer to those of monomers. The concentration of HRP was determined by its absorption at the Soret band ($\lambda_{403} = 1.02 \times 10^5\ M^{-1}cm^{-1}$ (25)). Protein thiol content was measured by Ellman's assay (λ_{412} = 14,150 $M^{-1}cm^{-1}$) (26, 27). The concentration of MR was estimated by the absorption of the FAD cofactor at 463 nm (ϵ = 11,300 $M^{-1}s^{-1}$) as previously (8).

Protein Thiol Alkylation by PEG-maleimide and Electrophoretic Analysis—Reaction mixtures (100 μl) containing reduced and/or oxidized *Mt*AhpE in the presence or absence of MSH, *Mt*Mrx1wt, or *Mt*Mrx1CXXA at indicated concentrations were precipitated by addition of 10 μl of trichloroacetic acid (TCA) (10% (w/v)) and kept on ice for 30 min. Protein precipitates were pelleted, washed with 100 μl of ice-cold acetone, dried at 37 °C, resuspended in 15 μl of 3 mM PEG-maleimide (in 50 mM Tris, 10 mM EDTA, 0.1% SDS, pH 7.5) and incubated at 45 °C for 45 min. Samples were immediately loaded on a 15% SDS-PAGE in the absence of β-ME, and proteins were stained with Coomassie Brilliant Blue.

Mass Spectrometrical Identification of Reaction Products—Protein samples were diluted to ~5 μM in 50% acetonitrile 0.1% acetic acid and intact protein mass measurements were performed by direct infusion in a microelectrospray ionization ion trap mass spectrometer (LTQ XL, ThermoFisher Scientific, San José, CA). The mass spectrometer was operated manually in positive ion mode with a source voltage set at 3.8 kV and the ion transfer tube at 220 °C The parent ions were submitted to in-source dissociation (SID) using the minimal energy to promote efficient declustering of water molecules and salts adducts. The mass spectra were deconvoluted using the software ProMass Deconvolution from ThermoFisher Scientific.

For the identification of *Mt*AhpE-*Mt*Mrx1CXXA mixed disulfide, the expected corresponding band was in-gel digested with sequencing grade trypsin (0.5 μg) overnight at 30 °C. The reaction was stopped by adding 0.1% trifluoroacetic acid. The peptides were analyzed by LC-MS/MS as described (28). The mass spectrometer was operated in the data-dependent-mode and switched automatically between MS, Zoom Scan for charge state determination and MS/MS for the most abundant ion. Each MS scan was followed by a maximum of five MS/MS using collision energy of 35%. Dynamic exclusion was enabled to allow analysis of co-eluting peptides. For peptide identification peak lists were generated using the application spectrum selector in the Proteome Discoverer 1.3 package. The resulting peak lists were searched using Sequest against a homemade protein database containing the *Mt*Mrx1 and *Mt*AhpE sequences (Uniprot Q8VJ51 and Q73YJ5). The following parameters were used: trypsin was selected with cleavage only after lysine and arginine; the number of internal cleavage sites was set to 1; the mass tolerance for precursor and fragment ions was 1.1 Da and 1.0 Da, respectively; and the considered dynamic modifications were +15.99 Da for oxidized methionine and +71.0 Da for acrylamide addition to cysteine. Peptide matches were filtered using charge-state *versus* cross-correlation scores (Xcorr). The mixed disulfide peptide between *Mt*Mrx1 and *Mt*AhpE was identified by the use of DBond software (29) and manually validated.

Rate Constant Determination of AhpE-mycothiol (AhpE-SS-M) Disulfide Formation—The kinetics of oxidized *Mt*AhpE reaction with mycothiol to form the mixed disulfide described above was determined by a competition approach, following *Mt*AhpE overoxidation to sulfinic acid by excess H_2O_2 in the absence and presence of mycothiol, which does not compete for initial oxidation of the peroxidatic cysteine due to the high rate constant of the latter enzyme. Overoxidation was measured following the accompanying intrinsic fluorescence increase, using an Aminco Bowman Series 2 luminescence spectrophotometer as previously (22), as in Equation 3.

$$\text{AhpE-SO}^- + \text{H}_2\text{O}_2 \rightarrow \text{AhpE-SO}_2^- + \text{H}_2\text{O} \qquad \text{(Eq. 3)}$$

Reduced *Mt*AhpE (2 μM) was mixed with H_2O_2 (150 μM) in the absence or presence of MSH (11–33 μM) producing a rapid decrease in the enzyme intrinsic fluorescence intensity, corresponding to its oxidation to sulfenic acid ($k = 8.2 \times 10^4\ M^{-1}\ s^{-1}$, reaction half-life under this conditions is ~0.06 s), followed by an increase in fluorescence corresponding to the enzyme overoxidation (k_1 = 40 $M^{-1}\ s^{-1}$, reaction half-life under this conditions is 115 s), as reported previously (22). Observed rate constants of fluorescence increase (k_{obs}) were determined by fitting experimental data to single exponentials. In the presence of mycothiol, in Equation 4,

$$k_{obs} = k_1 \times [\text{H}_2\text{O}_2] + k_2[\text{MSH}] \qquad \text{(Eq. 4)}$$

where k_2 is the second order rate constant for the reaction between oxidized *Mt*AhpE and reduced mycothiol. k_2 at pH 7.4 and 25 °C was obtained from the slope of k_{obs} *versus* MSH concentration, and the offset corresponds to $k_1 \times [H_2O_2]$.

Reduction of MtAhpE-SS-M by MtMrx1wt—Reaction mixtures containing reduced *Mt*AhpE (20 μM) were treated with mycothiol disulfide (MSSM, 20 μM) or oxidized with an equimolar concentration of H_2O_2. Immediately after oxidation, reduced MSH was added to reach a final concentration of 20 μM and incubated for 30 min to form *Mt*AhpE-SS-M. Time of incubation was selected to allow ≥90% mixed disulfide formation as calculated using Gepasy 3 software (30) and the rate constant of the reaction reported below. Then, *Mt*Mrx1 wt was added to one of the *Mt*AhpE-SS-M containing samples (20 μM Mrx1 and 10 μM *Mt*AhpE-SS-M final concentrations). After 15 min, samples were precipitated with TCA and analyzed by alkylation with PEG-maleimide.

Reduction of MtAhpE-SOH by MtMrx1wt—Oxidized *Mt*AhpE was prepared by incubation of reduced *Mt*AhpE (17 μM) with an

equimolar concentration of H_2O_2 for 1 min immediately after the oxidation step, reduced *Mt*Mrx1 was added to reach a final concentration of 16 μM *Mt*Mrx1 and 10 μM *Mt*AhpE. Aliquots (90 μl) were taken at different times of incubation (0.2, 0.5, and 4 min) and were directly added into tubes containing 10 μl of 100% TCA to stop the reaction and to precipitate the proteins. Samples before H_2O_2 addition (reduced *Mt*AhpE) and after oxidation and before *Mt*Mrx1 addition (oxidized *Mt*AhpE) were used as positive and negative controls, respectively. Samples were analyzed by alkylation with PEG-maleimide.

Reaction of Oxidized MtAhpE with the Nucleophilic Thiol in MtMrx1—Reaction mixtures containing reduced *Mt*AhpE (10 μM) in the absence or presence of *Mt*Mrx1wt or *Mt*Mrx1CXXA (30 μM) were treated with H_2O_2 (10 μM). After 15 min, TCA was added, and samples were analyzed by SDS-PAGE.

Reaction of MtAhpE-SS-M with MtMrx1wt or MtMrx1CXXA—Reaction mixtures containing reduced *Mt*AhpE (16 μM) in the absence or presence of MSH (30 μM) were treated with H_2O_2 (16 μM), to form *Mt*AhpE-SOH and *Mt*AhpE-SS-M, respectively. After 30 min, *Mt*Mrx1 wt or *Mt*Mrx1CXXA was added (20 μM *Mt*Mrx1wt or CXXA and 10 μM *Mt*AhpE-SOH or *Mt*AhpE-SS-M final concentrations). After 30 min, 10 mM NEM was added and incubated for 15 min, and samples were analyzed by SDS-electrophoresis in the absence of reductant.

Kinetics of Reaction of Oxidized MtAhpE with the Nucleophilic Thiol in MtMrx1CXXA—For the determination of the second-order rate constant of reaction between *Mt*AhpE-SOH and *Mt*Mrx1 CXXA, reaction mixtures containing 1 μM *Mt*AhpE and increasing concentrations of *Mt*Mrx1CXXA (10, 25 and 40 μM) were treated with 1 μM H_2O_2. Because of the high reactivity of the peroxidatic thiol in *Mt*AhpE (8×10^4 M^{-1} s^{-1} (22)) compared with the thiol groups of *Mt*Mrx1 (6.6 M^{-1} s^{-1}, see below), H_2O_2 is reduced by the former. 90-μl aliquots were taken at different time points and pipetted into Eppendorf tubes containing 10 μl of 100% TCA to stop the reaction and to precipitate the proteins. Samples were analyzed by SDS-PAGE, and Coomassie-stained gels were scanned in an Oddysey® LI-COR at 700 nm. Band intensity corresponding to the *Mt*AhpE-*Mt*Mrx1CXXA mixed disulfide (as identified by in gel digestion and mass spectrometry analysis, see below) was normalized against *Mt*Mrx1CXXA intensity, which was in ≥10-fold excess over *Mt*AhpE and therefore, should not be appreciably consumed during the assays. Relative disulfide intensity was plotted as a function of time, and plots were fitted to exponential growth curves. The second-order rate constant of the reaction of *Mt*AhpE-SOH with *Mt*Mrx1CXXA was obtained from the slope of the plot of the observed rate constants of mixed disulfide formation *versus Mt*Mrx1CXXA concentration.

Determination of the pK_a of the Thiols in Nucleophylic Cysteines of MtMrx1wt and CXXA—The pK_a of the nucleophilic cysteines of *Mt*Mrx1wt and the *Mt*Mrx1CXXA mutant were determined spectrophotometrically as described (31). Note that we used alkylated protein instead of oxidized (S-S) protein to correct for the background. The proteins were alkylated with 10 mM iodoacetamide for 30 min at room temperature. Excess of iodoacetamide was removed using size exclusion chromatography on Superdex75 10/300.

Kinetics of MtMrx1 Oxidation by H_2O_2—The intrinsic fluorescence intensity of *Mt*Mrx1 (λ_{exc} = 295 nm, λ_{em} = 335 nm) decreased upon oxidation by H_2O_2, in a way that was fully reversible by DTT-treatment. We took advantage of this spectral change to measure the kinetics of *Mt*Mrx1 reaction with H_2O_2, as previously reported for *Trypanosoma brucei* tryparedoxin 1 oxidation (32). Reduced *Mt*Mrx1 (10 μM) was mixed with an excess of H_2O_2 (0.25–1.0 mM) in an Aminco Bowman Series 2 luminescence spectrophotometer, and time courses of intrinsic fluorescence change were registered. Observed rate constants of fluorescence decrease (k_{obs}) were determined by fitting experimental data to single exponentials. The second order rate constant for the reaction between reduced *Mt*Mrx1 and H_2O_2 at pH 7.4 and 25 °C was obtained from the slope of the plot of k_{obs} *versus* H_2O_2 concentration.

Catalytic Consumption of H_2O_2 by MtAhpE in the Presence of MtMrx1—H_2O_2 was slowly delivered into solutions containing 2 μM *Mt*AhpE and/or reduced wild type or CXXA *Mt*Mrx1 (50 μM) using a motor-driven syringe system (KD Scientific) under continuous stirring (flux = 1 μM/min during 15 min). Aliquots of 20 μl were taken at different times and directly pipetted into plate wells (Fisherbrand® flat bottom well plate, clear) containing 180 μl of a solution of 1 μM HRP and 20 μM Amplex® red. H_2O_2-dependent Amplex® red oxidation was measured using a Fluostar BMG Lab plate fluorescence reader (λ_{ex} = 515 nm, λ_{em} = 590 nm). H_2O_2 concentration of each sample was determined according to appropriate calibration curves.

NADPH-dependent Peroxidase Activity in the Presence of MtMrx1 and MtAhpE—NADPH oxidation during *Mt*AhpE-mediated H_2O_2 reduction was determined using an enzyme-coupled assay. Briefly, reaction mixtures containing 100 μM NADPH, 20 μM reduced *Mt*AhpE, 5 μM reduced wt or CXXA *Mt*Mrx1, were incubated in 50 mM HEPES, 0.5 mM EDTA, pH 7.8 at 25 °C, followed by sequential addition of 0.13 μM *Cg*MR, 30 μM MSSM, and 20 μM H_2O_2. NADPH reduction was monitored at 340 nm (ϵ_{340} = 6,220 $M^{-1}cm^{-1}$) using a thermostated Shimadzu UV-2450 spectrophotometer. Reaction mixtures lacking *Mt*AhpE or *Mt*Mrx1 were used as negative controls.

RESULTS

Reaction of AhpE-SOH with MSH—When reduced *Mt*AhpE was incubated with an excess of PEG-maleimide and then analyzed by SDS-PAGE, a protein molecular weight shift of 5 kDa was observed, in agreement with the addition of one molecule of PEG/protein and the presence of one thiol per *Mt*AhpE monomer. As expected, this increase in the molecular weight was not observed when the enzyme was first oxidized to its sulfenic acid derivative by addition of equimolar H_2O_2, in agreement with specific alkylation of reduced cysteine residues (Fig. 1*A*). When oxidized *Mt*AhpE was incubated with reduced MSH, no thiol alkylation was observed, indicating that no reduction of AhpE-SOH by MSH took place (Fig. 1*A*). However, incubation with MSH did protect *Mt*AhpE from oxidation-dependent dimerization, a slow process that takes place after initial sulfenic acid formation (22). Considering that AhpE-SOH reacts with glutathione and *N*-acetylcysteine to form mixed disulfides, we hypothesized that protection was due to the formation of an *Mt*AhpE-SS-M adduct according to Equation 5.

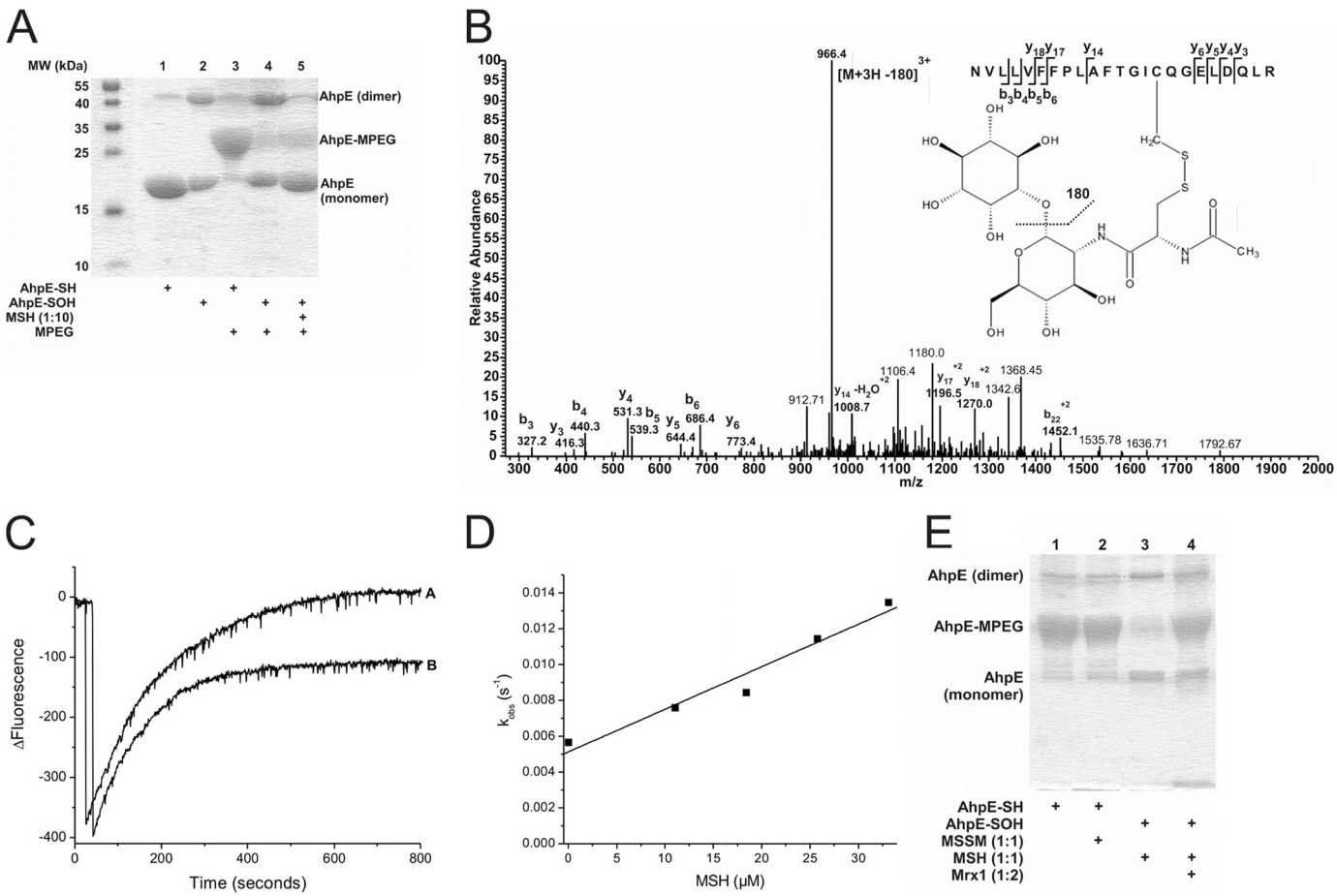

FIGURE 1. **Oxidized MtAhpE reacts with MSH forming a mixed disulfide that is reduced by MtMrx1.** *A*, alkylation of *Mt*AhpE with PEG-maleimide. Reduced or oxidized *Mt*AhpE (20 μM) was incubated with or without MSH (200 μM). Proteins were precipitated with TCA, treated with PEG-maleimide (5 mM), and evaluated on a CBB-stained 15% SDS-PAGE. *B*, identification of *S*-mycothiolation on cysteine 45 of *Mt*AhpE. Sample was obtained by adding MSH (60 μM) to oxidized *Mt*AhpE (20 μM). The LC-MS/MS spectrum shows data obtained from a 3+ parent ion with m/z = 1026.5. The spectrum displays one major daughter ion at m/z 966.4 corresponding to the neutral loss of inositol (180 Da) after fragmentation at a C-O bond. The *y*- and *b*- series of ions allowed exact localization of the mixed disulfide between mycothiol and the cysteine residue. *C*, kinetics of reaction of oxidized MtAhpE with MSH. Time-dependent decrease (oxidation) and increase (overoxidation) in the intrinsic fluorescence intensity (λ_{ex} = 295 nm, λ_{em} = 340 nm) of *Mt*AhpE (2 μM) in the absence (*A*) or presence (*B*) of MSH (18 μM) upon addition of H_2O_2 (150 μM) in 100 mM sodium phosphate buffer plus 0.1 mM DTPA. *D*, effect of the MSH concentration on the observed rate constants of *Mt*AhpE intrinsic fluorescence change caused by overoxidation. *E*, MtAhpE-SS-M reduction by MtMrx1. Reduced (*lanes 1* and *2*) or oxidized (*lanes 3* and *4*) *Mt*AhpE (20 μM) was incubated with MSSM (*lane 2*) or MSH (*lanes 3* and *4*)(20 μM) for 30 min, followed by incubation without (*lane 3*) or with *Mt*Mrx1 (*lane 4*) (20 μM) for 15 min. Samples were treated with PEG-maleimide (5 mM) and evaluated by CBB-stained 15% SDS-PAGE.

$$\text{AhpE-SOH} + \text{MSH} \rightarrow \text{AhpE-SS-M} + H_2O \quad \text{(Eq. 5)}$$

MS studies demonstrated the *S*-thiolation of *Mt*AhpE on cysteine 45 (Fig. 1*B*): the mass of the Cys-45 containing peptide was found to be 484 Da higher, consistent with the covalent attachment of MSH. Upon fragmentation of the precursor ion of m/z 1026.5 (z = 3), a predominant neutral loss of 180 Da was observed, corresponding to inositol and consistent with previous results (15). The LC-MS/MS spectrum also allowed exact localization of the mixed disulfide between mycothiol and the cysteine residue.

Kinetics of MtAhpE-SOH Reaction with Mycothiol—Incubation of reduced *Mt*AhpE with H_2O_2 in excess caused enzyme overoxidation to sulfinic acid, followed by the accompanying change in Trp fluorescence as previously described (22). After the addition of H_2O_2 in the presence of excess mycothiol, we observed a decrease in the amplitude and an increase in the observed rate constants (k_{obs}) of *Mt*AhpE overoxidation (Fig. 1*C*). The k_{obs} of the process linearly depended on the MSH concentration (Fig. 1*D*). The slope results in a second-order rate constant (k_2) of 237 $\pm$ 30 M^{-1} s^{-1} for the reaction of *Mt*AhpE-SOH with MSH at pH 7.4 and 25 °C. The offset corresponds to $k_1 \times [H_2O_2]$ and perfectly agrees with the previously determined rate constant of enzyme overoxidation (22).

Reduction of MtAhpE-SS-M by MtMrx1—When reduced *Mt*AhpE (20 μM) was incubated with mycothiol disulfide (MSSM, 20 μM) alkylation with PEG-maleimide was not abolished, indicating that at least under these conditions the reduced enzyme is not oxidized by the disulfide form of mycothiol. When *Mt*Mrx1 was added to pre-formed *Mt*AhpE-SS-M and further treated with PEG-maleimide, the protein was alkylated (Fig. 1*E*), indicating that *Mt*Mrx1 reduces *Mt*AhpE-SS-M.

Reduction of MtAhpE by MtMrx1—When oxidized *Mt*AhpE (10 μM) was incubated with reduced *Mt*Mrx1 (16 μM) for 0.2–4 min and further treated with PEG-maleimide, the enzyme was alkylated (Fig. 2*A*), indicating that *Mt*AhpE is reduced by *Mt*Mrx1 according to Equation 6.

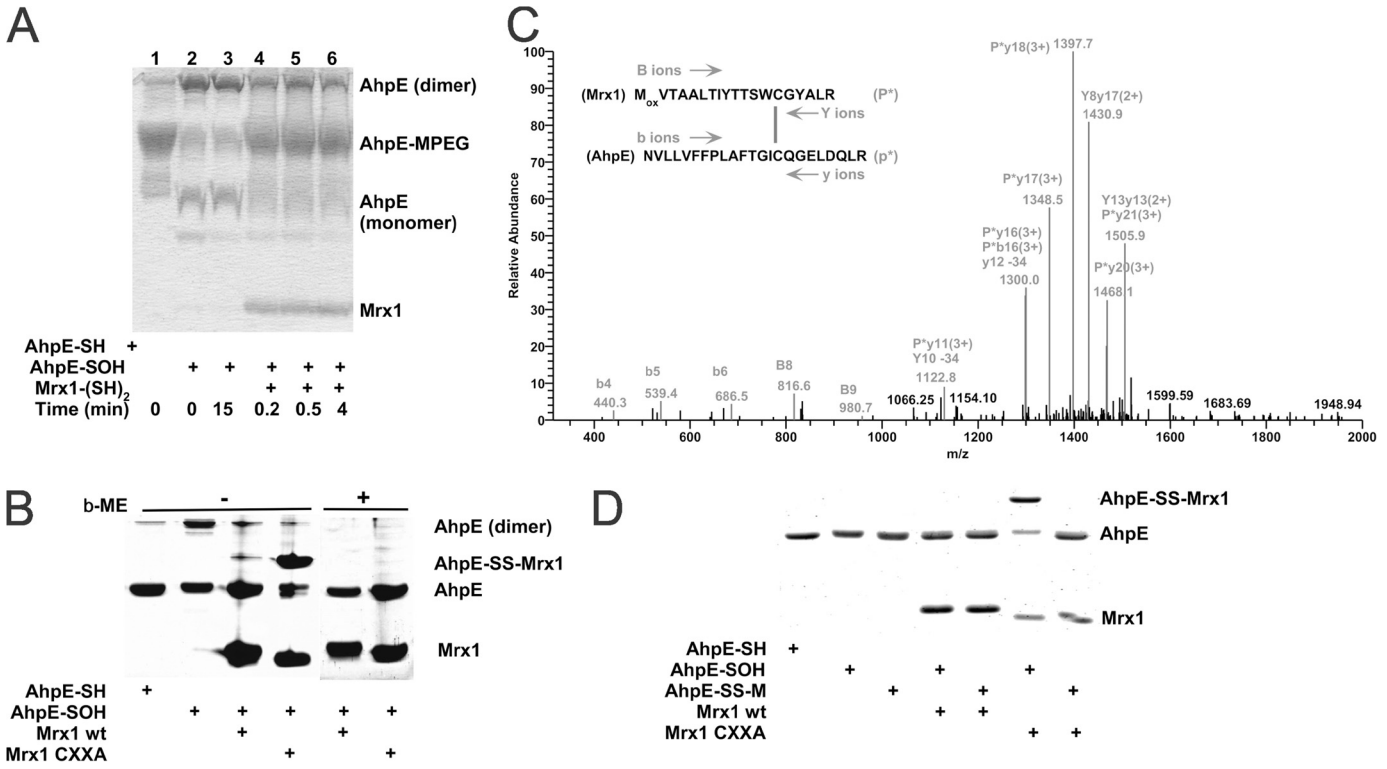

FIGURE 2. **MtAhpE is reduced by wild type MtMrx1 by a dithiolic mechanism.** *A*, reduced (*lane 1*) or oxidized (*lanes 2–6*) *Mt*AhpE (10 μM) incubated in the absence (*lanes 1–3*) or presence of reduced *Mt*Mrx1 (16 μM) for indicated times (*lanes 4–6*) and treated with 5 mM PEG-maleimide were evaluated on a Coomassie Brilliant Blue (CBB) stained 15% SDS-PAGE. *B*, reduced and oxidized *Mt*AhpE alone (10 μM), or oxidized *Mt*AhpE incubated with *Mt*Mrx1 wt or *Mt*Mrx1 CXXA (30 μM) for 15 min were evaluated on a CBB-stained 15% SDS-PAGE in the absence (*lanes 1–4*, respectively) or presence (*lanes 4–8*, respectively) of β-ME. A novel band with a molecular mass compatible with a mixed disulfide formation between *Mt*AhpE and *Mt*Mrx1CXXA is indicated as *Mt*AhpE-SS-*Mt*Mrx1. *C*, mass spectrometric analysis of the *Mt*AhpE-SS-*Mt*Mrx1 complex is shown in Fig. 2*B*. A quadruply charged parent ion of $[M+4H]^{4+} = 1183.7$ Da shows fragmentation characteristics of a disulfide linkage between Cys^{17} of *Mt*Mrx1 and Cys^{45} of *Mt*AhpE, as determined by the DBond software (29). *P**, one strand of a dipeptide; *p**, the other strand of a dipeptide; *capital letters*, fragment ions from peptide *P**; *lowercase letters*, fragment ions from peptide *p**. The loss of 34 atomic mass units represents formation of dehydroalanine from C-S bond fragmentation. *D*, reaction of *Mt*AhpE-SS-M with *Mt*Mrx1CXXA does not form a protein-protein intermolecular mixed disulfide. Reduced (*lane 1*) and oxidized *Mt*AhpE (*lanes 2–7*) alone (*lanes 2*, *4*, and *6*), or incubated with MSH during 30 min (*lanes 3*, *5*, and *7*), were incubated in the absence (*lanes 2* and *3*) or presence of *Mt*Mrx1 wt (*lanes 4* and *5*) or *Mt*Mrx1CXXA (*lanes 6* and *7*) for 15 min. Reaction was stopped by addition of 5 mM NEM, and samples were evaluated on a CBB-stained 15% SDS-PAGE under non-reducing conditions. A novel band with a molecular mass compatible with a mixed disulfide formation between *Mt*AhpE and *Mt*Mrx1CXXA is indicated as *Mt*AhpE-SS-*Mt*Mrx1.

$$\text{AhpE-SOH} + \text{Mrx1-(SH)}_2 \rightarrow \text{AhpE-SH} + \text{Mrx1-S}_2 + \text{H}_2\text{O} \quad \text{(Eq. 6)}$$

*Mt*Mrx1-dependent reduction of *Mt*AhpE was ~50% complete after 0.2–0.5 min, suggesting a relatively fast reaction. Interestingly, the addition of *Mt*Mrx1 partially inhibits the dimerization of *Mt*AhpE, which slowly occurs after oxidation (Fig. 2*A*).

Di- versus mono-thiolic Reduction of MtAhpE by MtMrx1—In *C. glutamicum* Mrx1, only the N-terminal cysteine residue of the CXXC active site sequence motif was found to be essential for the reduction of the arsenate-mycothiol adduct intermediate (16, 33). For the *Mt*Mrx1, however, the C-terminal cysteine mutated to alanine (*Mt*Mrx1 CXXA) was not able to reduce *Mt*AhpE. It formed a mixed disulfide (*Mt*AhpE-*Mt*Mrx1 CXXA), which was reducible by β-ME (Fig. 2*B*), indicating that both cysteine residues of *Mt*Mrx1 are essential for the reduction of *Mt*AhpE under these conditions, according to the following mechanism in Equations 7 and 8.

$$\text{AhpE-SOH} + \text{Mrx1-(SH)}_2 \rightarrow \text{AhpE-SS-Mrx1-SH} + \text{H}_2\text{O} \quad \text{(Eq. 7)}$$

$$\text{AhpE-SS-Mrx1-SH} \rightarrow \text{AhpE-SH} + \text{Mrx1-S}_2 \quad \text{(Eq. 8)}$$

Mass spectrometrical studies confirmed the mixed disulfide formation. A tryptic digest of the proteins present in the band corresponding to *Mt*AhpE-*Mt*Mrx1 CXXA in Fig. 2*B* revealed a mixed disulfide between two cysteine-containing tryptic peptides from each individual protein (Fig. 2*C*).

As above indicated, wild type *Mt*Mrx1 could directly reduce *Mt*AhpE-SOH (Fig. 2, *A* and *B*). Interestingly, when *Mt*Mrx1CXXA was added to *Mt*AhpE-SS-M, the AhpE-SS-Mrx1 mixed disulfide was not observed (Fig. 2*D*), indicating that the cysteine in *Mt*Mrx1CXXA reacts with the sulfur atom of MSH, yielding reduced *Mt*AhpE through the following reaction in Equation 9,

$$\text{AhpE-SS-M} - \text{Mrx1-SH} \rightarrow \text{AhpE-SH} + \text{Mrx1-SS-M} \quad \text{(Eq. 9)}$$

which is the reaction for a monothiolic mechanism of reduction.

Kinetics of MtAhpE-SOH Reaction with MtMrx1CXXA—When we oxidized *Mt*AhpE to its sulfenic acid derivative in the

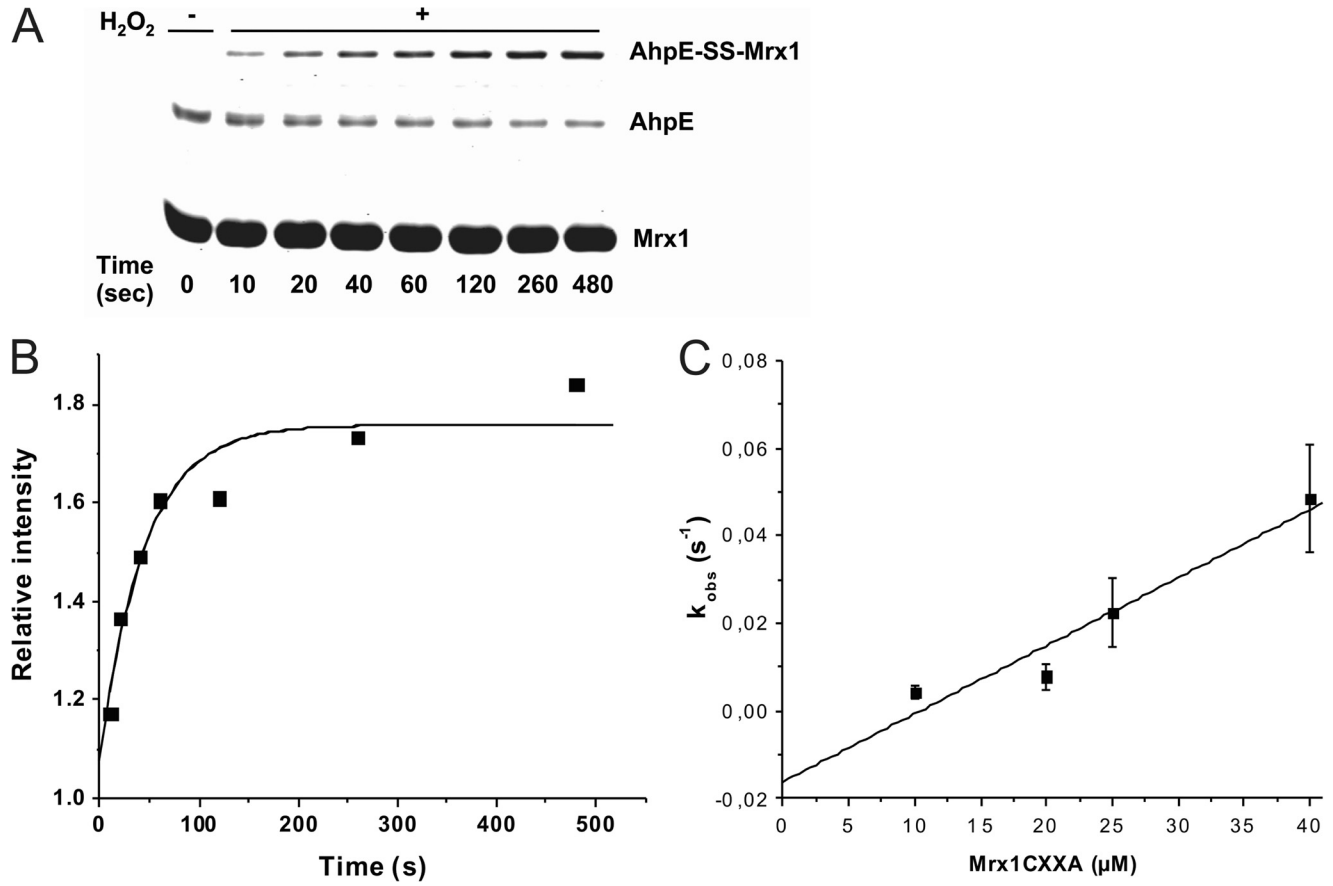

FIGURE 3. **Kinetics of the reaction of MtAhpE-SOH with the nucleophilic thiol in MtMrx1CXXA.** *A*, oxidized *Mt*AhpE (1 μM) was incubated with *Mt*Mrx1CXXA (25 μM), aliquots were taken at different incubation times and the reaction was stopped by addition of 10% TCA. Samples were evaluated on a CBB-stained 15% SDS-PAGE. *B*, time-dependent increase of the relative band intensity of the mixed disulfide shown in *A*, expressed as *Mt*AhpE-SS-*Mt*Mrx1/*Mt*Mrx1CXXA. *Mt*Mrx1CXXA in concentrations of more than 10 times excess remain constant, and was used as protein load control. The continuous line shows the best fit to an exponential curve. *C*, effect of increasing *Mt*Mrx1CXXA concentrations on the observed rate constants of intermolecular disulfide formation.

presence of excess *Mt*Mrx1CXXA, a time-dependent increase of the mixed disulfide between *Mt*AhpE and *Mt*Mrx1CXXA was observed (Fig. 3*A*). Time courses of formation of this mixed disulfide fitted to exponential curves (Fig. 3*B*), and the observed rate constants were dependent on the *Mt*Mrx1CXXA concentration (Fig. 3*C*). From the slope of the plot shown in Fig. 3*C*, a second-order rate constant, for the reaction between oxidized *Mt*AhpE and the N-terminal thiol in *Mt*Mrx1CXXA to form a mixed disulfide, of $(1.6 \pm 0.3) \times 10^3\ \text{M}^{-1}\ \text{s}^{-1}$ at pH 7.4 and 25 °C was determined.

pK_a Values of the Nucleophylic Cysteines in MtMrx1wt and MtMrx1CXXA—In previous work, we had determined the pK_a value of the nucleophilic cysteine residue of *Mt*Mrx1wt as 6.8 (15). To investigate the possible influence of the CXXA mutation on the reactivity of the nucleophilic cysteine, we determined the pK_a value of the nucleophilic cysteine of *Mt*Mrx1CXXA. We obtained a midpoint value of 7.6 (Fig. 4*A*).

Kinetics of MtMrx1 Thiol Oxidation by H_2O_2—When *Mt*Mrx1 (10 μM) was oxidized with H_2O_2 (1 mM), a time-dependent decrease in protein intrinsic fluorescence was observed in a way that was fully reversible by DTT treatment, indicating specificity for protein thiol oxidation (Fig. 4*B*). Time courses of fluorescence decay fitted to exponential curves, and observed rate constants were dependent on H_2O_2 concentrations (Fig. 4*C*). From the slope of the plot, a second-order rate constant for *Mt*Mrx1 oxidation by H_2O_2 of $(6.6 \pm 0.6)\ \text{M}^{-1}\ \text{s}^{-1}$ at pH 7.4 and 25 °C was obtained.

MtAhpE-catalyzed H_2O_2 Reduction via MtMrx1—We tested whether *Mt*AhpE was able to catalytically consume H_2O_2 in the presence of reduced *Mt*Mrx1. When a flux of H_2O_2 (1 μM min^{-1}) was infused to reduced *Mt*Mrx1 (50 μM), a time-dependent increase of H_2O_2 was observed (Fig. 5). After 15 min, nearly 14 μM H_2O_2 was accumulated, indicating that <10% of the H_2O_2 was consumed. This is consistent with a low reactivity of *Mt*Mrx1 toward H_2O_2 ($6.6 \pm 0.6\ \text{M}^{-1}\ \text{s}^{-1}$ at pH 7.4, Fig. 4*C*). Reduced *Mt*AhpE (2 μM) alone was not able to catalytically consume H_2O_2. However, when the same flux of H_2O_2 was infused to a mixture containing both reduced *Mt*Mrx1 and *Mt*AhpE, a much slower increase in H_2O_2 concentration was observed: 2.8 μM H_2O_2 accumulated after 15 min, indicating that 81% of the infused H_2O_2 has been consumed (Fig. 5). Importantly, while *Mt*AhpE catalytically consumed H_2O_2 in the presence of wt *Mt*Mrx1, the peroxidase activity of *Mt*AhpE abolished when the *Mt*Mrx1CXXA variant was used, once again indicating that both cysteine residues of *Mt*Mrx1 are essential for direct *Mt*AhpE reduction (Fig. 5).

MtAhpE Catalyzes the H_2O_2-dependent NADPH Oxidation—The addition of MSSM (30 μM) to a reaction mixture containing NADPH (100 μM), reduced *Mt*AhpE (20 μM), reduced *Mt*Mrx1 wt (5 μM), and *Cg*MR (0.13 μM) caused a rapid

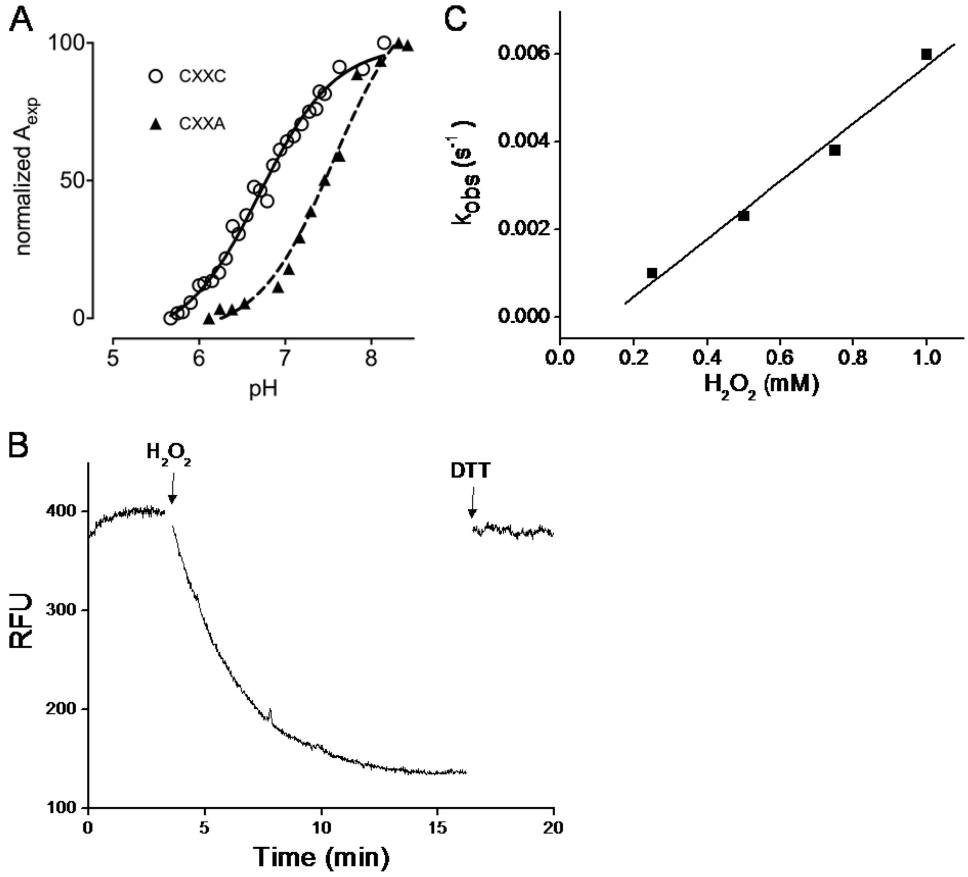

FIGURE 4. **MtMrx1 thiol pK_a determinations and kinetics of oxidation by H_2O_2.** *A*, pK_a titration curves for wild type (*circles*) (15) and the CXXA mutant (*triangles*). The specific absorption of the thiolate ion at 240 nm as a function of the pH is shown. A_{exp} is determined as described (31). Data were fitted with the Henderson-Hasselbach equation. *B*, time-dependent decrease in the total intrinsic fluorescence intensity (λ_{ex} = 295 nm, λ_{em} = 335 nm) of *Mt*Mrx1wt (10 μM) upon oxidation by H_2O_2 in 100 mM sodium phosphate buffer plus 0.1 mM DTPA, at pH 7.4 and room temperature. The *first arrow* indicates the addition of excess H_2O_2 (1.5 mM) and the second, the addition of DTT (1.5 mM). *C*, effect of H_2O_2 concentration on the observed rate constants of wt*Mt*Mrx1 intrinsic fluorescence change.

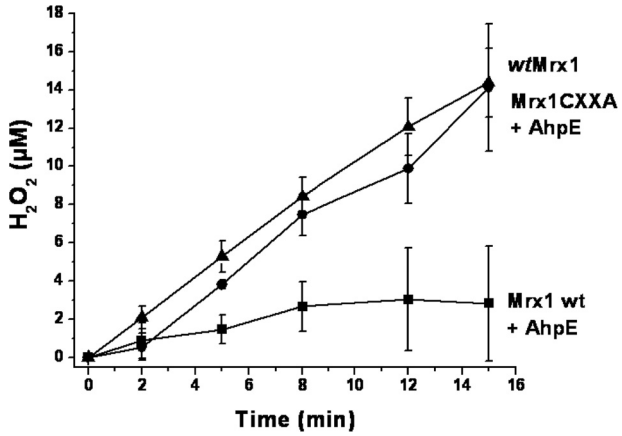

FIGURE 5. **MtAhpE catalyzes H_2O_2 reduction in the presence of MtMrx1.** H_2O_2 was infused (J = 1 μM min^{-1}) to reaction mixtures containing 50 μM reduced *Mt*Mrx1 wt (*triangles*), 50 μM reduced *Mt*Mrx1 CXXA + 2 μM *Mt*AhpE (*circles*), or 50 μM reduced *Mt*Mrx1 wt + 2 μM *Mt*AhpE (*squares*). Remaining H_2O_2 was measured at different time points, using Amplex®red oxidation assay. Data points represent an average of $n = 3 \pm$ S.D.

decrease in NADPH concentration, coupled to the reduction of MSSM, after which the absorbance remained constant. Subsequent addition of H_2O_2 (20 μM) led to an acceleration of NADPH consumption (1.6 ± 0.1 μM/min) indicating that the complete system supports a NADPH-dependent peroxidase activity (Fig. 6, *A* and *B*). This acceleration was not seen in the absence of *Mt*Mrx-1 or *Mt*AhpE. Notably, even when the CXXA mutant instead of wt *Mt*Mrx-1 was used, a H_2O_2-dependent acceleration of NADPH consumption was observed, although to a lower extent (~65% with respect to wt *Mt*Mrx-1)(Fig. 6*B*).

DISCUSSION

In previous work, we demonstrated the peroxidase activity of the one-cysteine peroxiredoxin from *M. tuberculosis*, *Mt*AhpE, using different peroxides and artificial reducing substrates. We found peroxynitrite and fatty acid hydroperoxides as preferential oxidizing substrates for this enzyme (22, 23), which interestingly was found associated to the membrane fraction of the bacterium (34). We have also proposed and used *Mt*AhpE as a model to study the mechanisms of cysteine residues oxidation (from thiol to sulfenic acid) and overoxidation (from sulfenic to sulfinic acid) in proteins (23). However, the identification of a biologically relevant reducing pathway to complete its catalytic cycle was lacking so far.

In the present work, we demonstrate that MSH is not able to reduce the sulfenic derivative of *Mt*AhpE, but forms a mixed disulfide with the enzyme, as confirmed by mass spectrometry (Fig. 1, *A* and *B*), with a rate constant of 237 $M^{-1}s^{-1}$ at pH 7.4 and 25 °C (Fig. 1, *C* and *D*). Mycoredoxin-1 was able to reduce the mixed disulfide formed between the enzyme and mycothiol

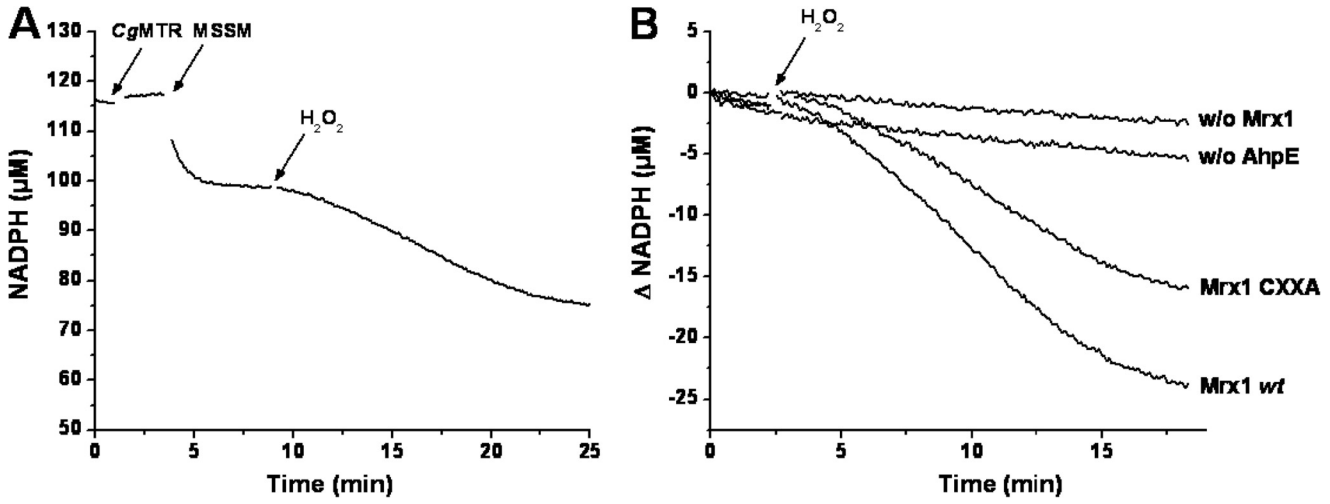

FIGURE 6. **NADPH consumption during MtAhpE-mediated H_2O_2 reduction.** *A*, time-dependent consumption of NADPH (100 μM) in a coupled assay containing 20 μM *Mt*AhpE, 5 μM *Mt*Mrx1*wt*, 0.13 μM *Cg*MR, 30 μM MSSM, and 20 μM H_2O_2 in 50 mM HEPES, 0.5 mM EDTA, pH 7.8 at 25 °C. The *arrows* indicate the addition of the last three mentioned components to the mixture. *B*, NADPH consumption upon addition of H_2O_2 (*arrow*) in mixtures as in *A* (Mrx1 wt); with CXXA instead of *wt Mt*Mrx1 (Mrx1 CXXA); in the absence of *Mt*Mrx1 (w/o Mrx1) or in the absence of *Mt*AhpE (w/o AhpE). Representative traces that were repeated in independent days with the same results are shown.

(Fig. 1*E*). The second thiol moiety of *Mt*Mrx1 was not needed for *Mt*AhpE-SS-M reduction, as indicated by the lack of detection of *Mt*AhpE-S-S-*Mt*Mrx1 adduct upon incubation with the *Mt*Mrx1CXXA mutant (Fig. 2*D*). Moreover the catalytic consumption of NADPH by a coupled assay consisting of NADPH/*Cg*MR/MSH/*Mt*Mrx1/*Mt*AhpE/H_2O_2 was also functional when *Mt*Mrx1 was substituted for *Mt*Mrx1 CXXA (Fig. 6*B*). These results are consistent with the reported data for *Cg*Mrx1-dependent reduction of arsenate by *Cg*ArsC1 and *Cg*ArsC2. In these enzymes, the proposed mechanism of reaction involves the initial formation of an arseno (V)-sulfur complex, followed by a nucleophilic attack by MSH resulting in a arseno mycothiol (As(V)-MSH) complex. Mrx1 reacts with the latter, releasing As(III) and forming a mixed disulfide with MSH which is then reduced by a second molecule of MSH yielding reduced Mrx1 and mycothiol disulfide. For *Mt*AhpE-SS-M reduction by *Mt*Mrx1, we propose an analogous monothiolic mechanism (16, 33), as illustrated in Fig. 7 described below.

We also showed that *Mt*Mrx1 reduces oxidized *Mt*AhpE as shown by thiol alkylation assays (Fig. 2*A*). However, a mutant form of *Mt*Mrx1 where the C-terminal cysteine was substituted for alanine (*Mt*Mrx1CXXA) forms a mixed disulfide with oxidized *Mt*AhpE, which was evidenced on SDS-PAGE (Fig. 2*B*) and peptide identification by mass spectrometry (Fig. 2*C*). Thus, the sulfenic acid at the peroxidatic cysteine in oxidized *Mt*AhpE reacts with the N-terminal Cys residue in *Mt*Mrx1, which is subsequently reduced by the second thiol moiety present in wild type *Mt*Mrx1, regenerating reduced *Mt*AhpE. Accordingly, wild type but not CXXA *Mt*Mrx1 supports the catalytic consumption of fluxes of H_2O_2 by *Mt*AhpE (Fig. 5). To note, reduced *Mt*Mrx1 caused a marginal H_2O_2 consumption in the absence of *Mt*AhpE, in agreement with the lack of peroxidase activity of *Mt*Mrx1 previously reported (15), and consistent with the rate constant of the reaction determined herein ($6.6 \pm 0.6\ M^{-1}s^{-1}$ at pH 7.4, Fig. 4). This value agrees with the quite low nucleophilic cysteine pK_a value (6.8) previously

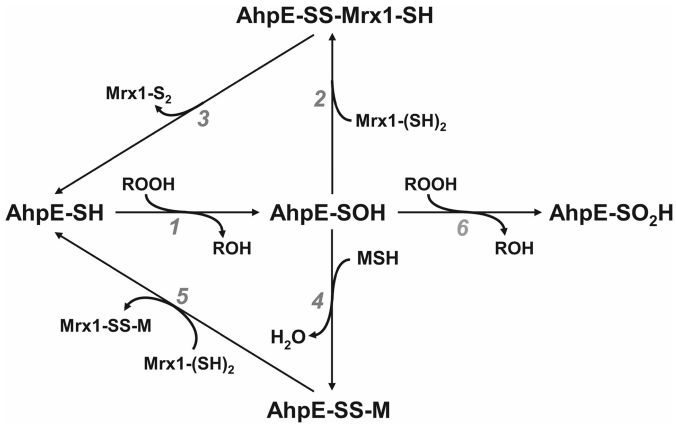

FIGURE 7. **Mechanisms proposed for MSH/Mrx1-dependent MtAhpE reduction.** *Mt*AhpE is oxidized by the peroxide to form a sulfenic acid (*reaction 1*). Sulfenic acid is then directly reduced by *Mt*Mrx1 (*reactions 2* and *3*), or through an intermediate disulfide formation with mycothiol (*reaction 4*), followed by reduction by *Mt*Mrx1 (*reaction 5*). The leaving Mrx1-S_2 and Mrx1-SS-M disulfide species are then reduced by a second mycothiol molecule forming mycothiol disulfide (MSSM) and reduced *Mt*Mrx1 as reported (7, 15). The formed MSSM is in turn reduced by the NADPH dependent flavoenzyme, mycothiol disulfide reductase (MR), as previously reported (8, 15). Both reducing pathways may compete with enzyme oxidative inactivation (overoxidation) to a sulfinic acid (*reaction 6*). The lower pathway (*reactions 4–5*) would predominate in the cytosol while the upper one (*reactions 2–3*) could be favored in membrane-associated compartments due to the hydrophilic nature of MSH.

reported (15), and pH-independent rate constants of thiolate oxidation by H_2O_2 in the 18–26 $M^{-1}s^{-1}$ range (35).

The *Mt*Mrx1CXXA mutant was used to estimate the second-order rate constant of the reaction between the sulfenic acid of *Mt*AhpE and the nucleophilic cysteine in *Mt*Mrx1 as $(1.6 \pm 0.3) \times 10^3\ M^{-1}s^{-1}$ at pH 7.4 (Fig. 3). This value is similar to that determined for the reaction between the sulfenic acid of *Mt*AhpE and the aromatic thiolate thionitrobenzoate ($(1.5 \pm 0.3) \times 10^3\ M^{-1}s^{-1}$ at pH 7.4 (22)) and higher than that determined for enzyme reduction by DTT ($90\ M^{-1}s^{-1}$, at pH 7.4 (23)). The rate constant determined this way is that of the first step leading to *Mt*AhpE reduction (Equation 8) and relies on a

mutant with potentially altered properties. In this respect, the pK_a value of the nucleophilic cysteine in *Mt*Mrx1CXXA is 7.6, which is 0.8 pH units higher than that of *Mt*Mrx1wt (Fig. 4*A*). Thus, the nucleophilic thiol is 80% deprotonated at pH 7.4 for *Mt*Mrx1wt and only 40% for its CXXA mutant, which could result in a ~50% lower reactivity at physiological pH. The rate constant obtained using this mutant is most probably a lower limit for the rate-limiting step during the overall process (Equation 7), since experiments using wild type *Mt*Mrx1 (16 μM) showed an important fraction of *Mt*AhpE (10 μM) reduction (≥50%) in only 0.2–0.5 min (Fig. 2*A*), which is consistent with a global rate constant of reduction in the ~10^3-10^4 $M^{-1}s^{-1}$ range according to computer-assisted simulations using Gepasy 3 software. When comparing with reduction of other *Mt*Prxs by thioredoxins, *Mt*Mrx-1-catalyzed *Mt*AhpE reduction seems to approach the reported rate constant of thioredoxin-mediated reduction of other Prxs (*Mt*TPx or *Mt*AhpC), which occur with rate constants in the 10^4 $M^{-1}s^{-1}$ range (13, 36). The rate constant of *Mt*AhpE reduction by *Mt*Mrx1 is ~10-fold higher than that of mixed disulfide formation with mycothiol (Fig. 1, *C* and *D*). However, as mentioned above, the concentration of mycothiol is in the millimolar range in the *M. tuberculosis* cytosolic fraction (6) and therefore, to effectively compete with mycothiol for oxidized *Mt*AhpE, the *Mt*Mrx1concentration (which is unknown so far) should be ≥50 μM. As indicated, proteomic analysis found *Mt*AhpE in the membrane-associated fraction. Direct *Mt*Mrx1-dependent *Mt*AhpE reduction might be favored in these hydrophobic compartments that are difficult to reach for a polar molecule, such as MSH. In any case, both direct reduction by *Mt*Mrx1 and mixed disulfide formation with mycothiol are fast enough to compete with H_2O_2-mediated enzyme oxidative inactivation (rate constant of 40 $M^{-1}s^{-1}$) (Figs. 3*C* and 1*D*, respectively). Whether *Mt*AhpE oxidative inactivation can compete with enzyme reduction by MSH/*Mt*Mrx1 *in vivo* will not only depend on the rate constants of reactions, but also on the steady-state concentrations of reducing as well as oxidizing substrates.

*Mt*AhpE reduction by the MSH/Mrx-1 system led to mycothiol oxidation that was reduced by *Cg*MR as indicated by the NADPH consumption observed using a coupled assay shown in Fig. 6. No NADPH-dependent peroxidase activity occurred in the absence of *Mt*AhpE. This was also true in the absence of *Mt*Mrx-1, indicating that oxidized *Mt*AhpE or the mixed disulfide *Mt*AhpE-SM adduct could not be reduced directly by MR/NADPH. Moreover, *Mt*Mrx1CXXA had 65% of the activity measured using *Mt*Mrx1wt, indicating that in the presence of mycothiol most *Mt*AhpE reduction occurs through a monothiolic mechanism. These results are in agreement with the lack of AhpE-Mrx1CXXA adduct detection by SDS-PAGE in the presence of mycothiol (Fig. 2*D*, *lane 7*). To our knowledge, this is the first identification of a biologically relevant reducing enzyme for this one-cysteine peroxiredoxin from *M. tuberculosis* or any other member of the AhpE family of Prxs. It is also the first report on the reduction of a mycothiol-containing protein mixed disulfide by Mrx1 from Mycobacteria. Moreover, the data reported herein specifies a molecular link between a peroxidase system and the mycothiol/mycoredoxin-1 pathway in Mycobacteria. We propose a mechanism of peroxide sensing and/or detoxification (Fig. 7) where *Mt*AhpE is oxidized by the peroxide to form a sulfenic acid (Fig. 7, *reaction 1*). The sulfenic acid is then directly reduced by *Mt*Mrx1 (Fig. 7, *reactions 2* and *3*), by a dithiolic mechanism involving a *Mt*AhpE-SS-*Mt*Mrx1 intermediate. Alternatively, disulfide formation with MSH followed by reduction by *Mt*Mrx1 occurs (Fig. 7, *reactions 4* and *5*). In any case, the leaving *Mt*Mrx1-S_2 and *Mt*Mrx1-SS-M disulfide are then reduced by mycothiol (7, 15) which in turn is maintained in its reduced state by mycothiol disulfide reductase (MR) at the expense of NADPH (8). Both reducing pathways compete with enzyme overoxidation to sulfinic acid (Fig. 7, *reaction 6*). To note, glutaredoxins from different cellular sources have been reported to be involved in homologous Prxs reduction and both monothiolic and dithiolic mechanisms have been proposed (37–41).

A recent report using thiol redox proteomic and mass spectrometry to identify *S*-mycothiolated proteins in *C. glutamicum* during NaOCl stress revealed that TPx was one of the proteins that is modified on its thiols. *S*-Mycothiolation affected *Cg*TPx activity that was restored by incubation with *Cg*Mrx1 (17). MSH/Mrx1-dependent reduction has not been described in other Prxs from Mycobacteria (TPx and AhpC) studied so far, where NADPH/thioredoxin reductase is directly used to reduce different isoforms of thioredoxin, the reducing substrates for most of the bacterial Prxs (13, 18). For *Mt*AhpC, an alternative reducing system, based on dihydrolipoamide linked to metabolic enzymes, has been demonstrated (42). Mrx-1 was not evaluated as reducing substrate for other peroxiredoxins from *M. tuberculosis* (Bcp and BcpB) so far.

Thioredoxins, tryparedoxins, as well as different glutaredoxins and NrdH-redoxins, are known to reduce many other protein substrates besides thiol-dependent peroxidases, such as ribonucleotide reductases (43–45). Similarly, we propose that reduction of protein oxidized cysteine residues, either at the sulfenic acid or MSH-mixed disulfide state, by *Mt*Mrx1, may be not specific for *Mt*AhpE. Ongoing structural and functional studies on the *Mt*AhpE-Mrx1 adduct will help to understand the bases of the interaction, which could predict protein molecular features required for a dithiolic mechanism of Mrx1-dependent protein reduction to operate. Similarly, structural data regarding the *Mt*AhpE-SSM mixed disulfide could provide the basis for the identification of proteins susceptible to this modification, which, as glutathionylation in other cellular systems, may importantly affect protein function.

*Mt*Mrx1-dependent *Mt*AhpE reduction provides an explanation for the increased susceptibility to oxidative stress in strains of Mycobacteria lacking functional Mrx1 or with a low MSH content[8] (7–9, 11). Moreover, Prxs and other thiol-dependent peroxidases have recently been proposed as key mediators in peroxide signaling (46–48). The results shown herein, taken together with our previous reports establishing peroxynitrite and fatty acid hydroperoxides as preferential substrates for *Mt*AhpE (23), provide a possible route for sensing these peroxides in Mycobacteria (12). The importance of this metabolic

[8] Mrx1-deletion studies were performed in *M. smegmatis*, which contains an AhpE with 71% protein identity to *Mt*AhpE according to PeroxiBase (20).

pathway *in vivo* and its possible consequences on infectivity and pathogenesis will be the subject of future investigations.

Acknowledgments—We thank Dr. E. Paek (Hanyang University, Korea) for help with the use of DBond software and Gaetan Herinckx for experimental assistance.

REFERENCES

1. World Health Organization. (2012) Global Tuberculosis Report
2. Nathan, C. (2009) Taming tuberculosis: a challenge for science and society. *Cell Host Microbe.* **5,** 220–224
3. Alvarez, M. N., Peluffo, G., Piacenza, L., and Radi, R. (2011) Intraphagosomal peroxynitrite as a macrophage-derived cytotoxin against internalized Trypanosoma cruzi: consequences for oxidative killing and role of microbial peroxiredoxins in infectivity. *J. Biol. Chem.* **286,** 6627–6640
4. Fang, F. C. (2004) Antimicrobial reactive oxygen and nitrogen species: concepts and controversies. *Nat. Rev. Microbiol.* **2,** 820–832
5. Nathan, C., and Shiloh, M. U. (2000) Reactive oxygen and nitrogen intermediates in the relationship between mammalian hosts and microbial pathogens. *Proc. Natl. Acad. Sci. U.S.A.* **97,** 8841–8848
6. Newton, G. L., and Fahey, R. C. (2002) Mycothiol biochemistry. *Arch. Microbiol.* **178,** 388–394
7. Van Laer, K., Hamilton, C. J., and Messens, J. (2013) Low-molecular-weight thiols in thiol-disulfide exchange. *Antioxid. Redox Signal.* **18,** 1642–1653
8. Patel, M. P., and Blanchard, J. S. (1999) Expression, purification, and characterization of Mycobacterium tuberculosis mycothione reductase. *Biochemistry* **38,** 11827–11833
9. Rawat, M., Johnson, C., Cadiz, V., and Av-Gay, Y. (2007) Comparative analysis of mutants in the mycothiol biosynthesis pathway in *Mycobacterium smegmatis*. *Biochem. Biophys. Res. Commun.* **363,** 71–76
10. Rawat, M., Kovacevic, S., Billman-Jacobe, H., and Av-Gay, Y. (2003) Inactivation of mshB, a key gene in the mycothiol biosynthesis pathway in *Mycobacterium smegmatis*. *Microbiology* **149,** 1341–1349
11. Rawat, M., Newton, G. L., Ko, M., Martinez, G. J., Fahey, R. C., and Av-Gay, Y. (2002) Mycothiol-deficient Mycobacterium smegmatis mutants are hypersensitive to alkylating agents, free radicals, and antibiotics. *Antimicrob Agents Chemother* **46,** 3348–3355
12. Ta, P., Buchmeier, N., Newton, G. L., Rawat, M., and Fahey, R. C. (2011) Organic hydroperoxide resistance protein and ergothioneine compensate for loss of mycothiol in *Mycobacterium smegmatis* mutants. *J. Bacteriol.* **193,** 1981–1990
13. Jaeger, T., Budde, H., Flohé, L., Menge, U., Singh, M., Trujillo, M., and Radi, R. (2004) Multiple thioredoxin-mediated routes to detoxify hydroperoxides in *Mycobacterium tuberculosis*. *Arch. Biochem. Biophys.* **423,** 182–191
14. Cole, S. T., and Barrell, B. G. (1998) Analysis of the genome of *Mycobacterium tuberculosis* H37Rv. *Novartis Found Symp.* **217,** 160–172; discussion 172–167
15. Van Laer, K., Buts, L., Foloppe, N., Vertommen, D., Van Belle, K., Wahni, K., Roos, G., Nilsson, L., Mateos, L. M., Rawat, M., van Nuland, N. A., and Messens, J. (2012) Mycoredoxin-1 is one of the missing links in the oxidative stress defense mechanism of Mycobacteria. *Mol. Microbiol.* **86,** 787–804
16. Ordoñez, E., Van Belle, K., Roos, G., De Galan, S., Letek, M., Gil, J. A., Wyns, L., Mateos, L. M., and Messens, J. (2009) Arsenate reductase, mycothiol, and mycoredoxin concert thiol/disulfide exchange. *J. Biol. Chem.* **284,** 15107–15116
17. Chi, B. K., Busche, T., Laer, K. V., Basell, K., Becher, D., Clermont, L., Seibold, G. M., Persicke, M., Kalinowski, J., Messens, J., and Antelmann, H. (2013) Protein *S*-Mycothiolation Functions as Redox-Switch and Thiol Protection Mechanism in *Corynebacterium glutamicum* Under Hypochlorite Stress. *Antioxid. Redox Signal.*, In press
18. Hugo, M., Radi, R., and Trujillo, M. (2012) Thiol dependent peroxidases in *Mycobacterium tuberculosis* in *Understanding Tuberculosis: Deciphering the Secret Life of the Bacilli* (Cardona, P.-J., ed.), InTech. pp. 293–316
19. Soito, L., Williamson, C., Knutson, S. T., Fetrow, J. S., Poole, L. B., and Nelson, K. J. (2011) PREX: PeroxiRedoxin classification indEX, a database of subfamily assignments across the diverse peroxiredoxin family. *Nucleic Acids Res.* **39,** D332–337
20. Oliva, M., Theiler, G., Zamocky, M., Koua, D., Margis-Pinheiro, M., Passardi, F., and Dunand, C. (2009) PeroxiBase: a powerful tool to collect and analyse peroxidase sequences from Viridiplantae. *J. Exp. Bot.* **60,** 453–459
21. Li, S., Peterson, N. A., Kim, M. Y., Kim, C. Y., Hung, L. W., Yu, M., Lekin, T., Segelke, B. W., Lott, J. S., and Baker, E. N. (2005) Crystal Structure of AhpE from *Mycobacterium tuberculosis*, a 1-Cys peroxiredoxin. *J. Mol. Biol.* **346,** 1035–1046
22. Hugo, M., Turell, L., Manta, B., Botti, H., Monteiro, G., Netto, L. E., Alvarez, B., Radi, R., and Trujillo, M. (2009) Thiol and sulfenic acid oxidation of AhpE, the one-cysteine peroxiredoxin from *Mycobacterium tuberculosis*: kinetics, acidity constants, and conformational dynamics. *Biochemistry* **48,** 9416–9426
23. Reyes, A. M., Hugo, M., Trostchansky, A., Capece, L., Radi, R., and Trujillo, M. (2011) Oxidizing substrate specificity of *Mycobacterium tuberculosis* alkyl hydroperoxide reductase E: kinetics and mechanisms of oxidation and overoxidation. *Free Radic. Biol. Med.* **51,** 464–473
24. Hildebraundt, A. G., and Roots, I. (1975) Reduced nicotinamide adenine dinucleotide phosphate (NADPH) dependent formation and breakdown of hydrogen peroxide during mixed function oxidation reactions in liver microsomes. *Arch. Biochem. Biophys.* **171,** 385–397
25. Schonbaum, G. R., and Lo, S. (1972) Interaction of peroxidases with aromatic peracids and alkyl peroxides. Product analysis. *J. Biol. Chem.* **247,** 3353–3360
26. Ellman, G. L. (1959) Tissue sulfhydryl groups. *Arch. Biochem. Biophys.* **82,** 70–77
27. Riddles, P. W., Blakeley, R. L., and Zerner, B. (1979) Ellman's reagent: 5,5′-dithiobis(2-nitrobenzoic acid)–a reexamination. *Anal. Biochem.* **94,** 75–81
28. Pyr Dit Ruys, S., Wang, X., Smith, E. M., Herinckx, G., Hussain, N., Rider, M. H., Vertommen, D., and Proud, C. G. (2012) Identification of autophosphorylation sites in eukaryotic elongation factor-2 kinase. *Biochem. J.* **442,** 681–692
29. Choi, S., Jeong, J., Na, S., Lee, H. S., Kim, H. Y., Lee, K. J., and Paek, E. (2010) New algorithm for the identification of intact disulfide linkages based on fragmentation characteristics in tandem mass spectra. *J. Proteome Res.* **9,** 626–635
30. Mendes, P. (1993) GEPASI: a software package for modelling the dynamics, steady states and control of biochemical and other systems. *Comput. Appl. Biosci.* **9,** 563–571
31. Roos, G., Garcia-Pino, A., Van Belle, K., Brosens, E., Wahni, K., Vandenbussche, G., Wyns, L., Loris, R., and Messens, J. (2007) The conserved active site proline determines the reducing power of *Staphylococcus aureus* thioredoxin. *J. Mol. Biol.* **368,** 800–811
32. Piñeyro, M. D., Arcari, T., Robello, C., Radi, R., and Trujillo, M. (2011) Tryparedoxin peroxidases from *Trypanosoma cruzi*: high efficiency in the catalytic elimination of hydrogen peroxide and peroxynitrite. *Arch. Biochem. Biophys.* **507,** 287–295
33. Villadangos, A. F., Van Belle, K., Wahni, K., Dufe, V. T., Freitas, S., Nur, H., De Galan, S., Gil, J. A., Collet, J. F., Mateos, L. M., and Messens, J. (2011) *Corynebacterium glutamicum* survives arsenic stress with arsenate reductases coupled to two distinct redox mechanisms. *Mol. Microbiol.* **82,** 998–1014
34. Gu, S., Chen, J., Dobos, K. M., Bradbury, E. M., Belisle, J. T., and Chen, X. (2003) Comprehensive proteomic profiling of the membrane constituents of a *Mycobacterium tuberculosis* strain. *Mol. Cell Proteomics* **2,** 1284–1296
35. Winterbourn, C. C., and Metodiewa, D. (1999) Reactivity of biologically important thiol compounds with superoxide and hydrogen peroxide. *Free Radic Biol. Med.* **27,** 322–328
36. Trujillo, M., Mauri, P., Benazzi, L., Comini, M., De Palma, A., Flohé, L., Radi, R., Stehr, M., Singh, M., Ursini, F., and Jaeger, T. (2006) The mycobacterial thioredoxin peroxidase can act as a one-cysteine peroxiredoxin. *J. Biol. Chem.* **281,** 20555–20566
37. Rouhier, N., Gelhaye, E., and Jacquot, J. P. (2002) Glutaredoxin-dependent peroxiredoxin from poplar: protein-protein interaction and catalytic

mechanism. *J. Biol. Chem.* **277,** 13609–13614
38. Pedrajas, J. R., Padilla, C. A., McDonagh, B., and Bárcena, J. A. (2010) Glutaredoxin participates in the reduction of peroxides by the mitochondrial 1-CYS peroxiredoxin in *Saccharomyces cerevisiae*. *Antioxid Redox Signal* **13,** 249–258
39. Hanschmann, E. M., Lönn, M. E., Schütte, L. D., Funke, M., Godoy, J. R., Eitner, S., Hudemann, C., and Lillig, C. H. (2010) Both thioredoxin 2 and glutaredoxin 2 contribute to the reduction of the mitochondrial 2-Cys peroxiredoxin Prx3. *J. Biol. Chem.* **285,** 40699–40705
40. Reeves, S. A., Parsonage, D., Nelson, K. J., and Poole, L. B. (2011) Kinetic and thermodynamic features reveal that *Escherichia coli* BCP is an unusually versatile peroxiredoxin. *Biochemistry* **50,** 8970–8981
41. Reynolds, C. M., Meyer, J., and Poole, L. B. (2002) An NADH-dependent bacterial thioredoxin reductase-like protein in conjunction with a glutaredoxin homologue form a unique peroxiredoxin (AhpC) reducing system in *Clostridium pasteurianum*. *Biochemistry* **41,** 1990–2001
42. Bryk, R., Lima, C. D., Erdjument-Bromage, H., Tempst, P., and Nathan, C. (2002) Metabolic enzymes of mycobacteria linked to antioxidant defense by a thioredoxin-like protein. *Science* **295,** 1073–1077
43. Dormeyer, M., Reckenfelderbäumer, N., Ludemann, H., and Krauth-Siegel, R. L. (2001) Trypanothione-dependent synthesis of deoxyribonucleotides by *Trypanosoma brucei* ribonucleotide reductase. *J. Biol. Chem.* **276,** 10602–10606
44. Holmgren, A. (1979) Glutathione-dependent synthesis of deoxyribonucleotides. Characterization of the enzymatic mechanism of *Escherichia coli* glutaredoxin. *J. Biol. Chem.* **254,** 3672–3678
45. Van Laer, K., Dziewulska, A. M., Fislage, M., Wahni, K., Hbeddou, A., Collet, J. F., Versées, W., Mateos, L. M., Tamu Dufe, V., and Messens, J. (2013) NrdH-redoxin of *Mycobacterium tuberculosis* and *Corynebacterium glutamicum* dimerizes at high protein concentration and exclusively receives electrons from thioredoxin reductase. *J. Biol. Chem.* **288,** 7942–7955
46. Delaunay, A., Pflieger, D., Barrault, M. B., Vinh, J., and Toledano, M. B. (2002) A thiol peroxidase is an H2O2 receptor and redox-transducer in gene activation. *Cell* **111,** 471–481
47. Fomenko, D. E., Koc, A., Agisheva, N., Jacobsen, M., Kaya, A., Malinouski, M., Rutherford, J. C., Siu, K. L., Jin, D. Y., Winge, D. R., and Gladyshev, V. N. (2011) Thiol peroxidases mediate specific genome-wide regulation of gene expression in response to hydrogen peroxide. *Proc. Natl. Acad. Sci. U.S.A.* **108,** 2729–2734
48. Azevedo, D., Tacnet, F., Delaunay, A., Rodrigues-Pousada, C., and Toledano, M. B. (2003) Two redox centers within Yap1 for H2O2 and thiol-reactive chemicals signaling. *Free Radic Biol. Med.* **35,** 889–900